Available online at www.sciencedirect.com
SCIENCE DIRECT®
Journal of Solid State Chemistry 174 (2003) 233–240
JOURNAL OF SOLID STATE CHEMISTRY
http://elsevier.com/locate/jssc

On the structural and electronic properties of poly(dicarbon monofluoride): solid-state semi-empirical INDO study

Peter Pelikán,[a,b,✠] Jozef Noga,[c,d] and Stanislav Biskupič[a,*]

[a] Department of Physical Chemistry, Slovak University of Technology, Radlinského 9, SK-812 37 Bratislava, Slovak Republic
[b] Department of Physical Chemistry, Chemical Faculty, Technical University Brno, Purkyňova 118, CZ-612 00, Czech Republic
[c] Institute of Inorganic Chemistry, Slovak Academy of Sciences, Dúbravska cesta 9, SK-842 36 Bratislava, Slovak Republic
[d] Department of Physical and Theoretical Chemistry, Faculty of Science, Comenius University, Mlynská dolina CH1, SK-84215 Bratislava, Slovak Republic

Received 3 October 2002; received in revised form 12 February 2003; accepted 20 February 2003

Abstract

Three-dimensional semi-empirical quantum chemical calculations of the structural and electronic properties of the fluorine intercalated graphite compound poly(dicarbon monofluoride)—$(C_2F)_n$ have been performed for several possible stacking sequences of puckered *trans*-cyclohexane chair layers. Such basic structure consisting from carbon hexagons in chair conformation has been confirmed. Furthermore, based on the geometry optimization, 12 structural sequences have been found to provide a local minima on the potential hypersurface, from which four are considerably more stable and one can assume their statistical distribution in the real poly(dicarbon monofluoride). This is also indicated by comparison with recent $K\alpha$ XES spectra. In such arrangement the maximal entropy contribution leads to the minimum Gibbs energy of the system. Band structure calculations show that the most stable sequences have insulating properties, which implies that the real poly(carbon monofluoride) behaves as an insulator. The conductive properties of some less stable sequences result from particular interlayer interactions.

Keywords: Intercalated graphite; Poly(dicarbon monofluoride); Geometric structure; Band structure; Electric conductivity

1. Introduction

Graphite fluorides $(C_xF)_n$ are graphite/fluorine intercalation compounds with covalent C–F bonds, known to have remarkable properties (see Ref. [1] and references therein). Stoichiometric graphite fluorides, poly(carbon monofluoride), $(CF)_n$, usually named graphite monofluoride, and poly(dicarbon monofluoride), $(C_2F)_n$, are, for instance, exceptional lubricants but also excellent electrode materials in primary lithium batteries [2–4]. From this point of view $(C_2F)_n$ has received more attention since it has a higher discharge potential than $(CF)_n$. Structure and properties of $(CF)_n$ were studied in our former work [5]. Here we are going to focus our attention to $(C_2F)_n$.

Single layers of $(C_2F)_n$, as well as that of $(CF)_n$, are considered to be puckered consisting of *trans*-cyclohexane chairs, which corresponds to experimentally determined hexagonal structure [1]. Moreover, *cis–trans*-linked cyclohexane boats are unlikely in $(C_2F)_n$, as to bond three fluorine atoms in the three next neighbor's carbon atoms of the cyclohexane ring is practically impossible.

Formation of the graphite fluorides proceeds as a diffusion process when C–F covalent bonds are created during the diffusion of fluorine atoms into the graphite bulk [1]. Graphite, from which the fluorinated graphite originates, can have three possible sequences of individual layers AAAA, ABAB, and ABCABC [6], the latter being quite rare. Accordingly, the same types of sequences can be expected in the intercalated graphite compounds. Hence, it is natural to assume that the most important and most frequent sequences in fluorinated graphite will again be those of AAAA or ABAB types to which we will focus in this work. Other possible structures may have mirror planes parallel with carbon sheets and perpendicular to the *c*-axis, sometimes also twin crystal result in the process of poly(dicarbon

*Corresponding author.
E-mail address: biskupic@cvt.stuba.sk (S. Biskupič).
✠ Deceased.

0022-4596/03/$ - see front matter © 2003 Elsevier Inc. All rights reserved.
doi:10.1016/S0022-4596(03)00132-4

monofluoride) formation. Thus, in poly(dicarbon monofluoride) as a polycrystal, various types of the arrangements of individual layers may arise whose experimental determination from X-ray diffraction data is an overwhelming problem, because of the difficulty to synthesize a sufficiently big monocrystal of this compound [1].

In 1979 Kita et al. [7] claimed the existence of a fluorine-graphite intercalation compound $(C_2F)_n$ of stoichiometric composition. The authors regarded the diffraction spots as those with two-fold symmetry and proposed a monoclinic structure of $(C_2F)_n$. Formerly, such a structure model was suggested to have an orthorhombic unit cell [1].

Fujii [8] attempted to evaluate the (*hk*0) diffraction spots more precisely by X-ray and electron diffraction and confirmed that $(C_2F)_n$ has the six-fold symmetry, like $(CF)_n$. His suggestion for the structure was considerably different from those of *conventional* graphite compounds. C–F bonds perpendicular to the carbon sheets linked the two layers of cyclohexane chairs. Fluorine atoms were bonded to tertiary carbons from above and from below of the double carbon sheets. The double carbon layer model belongs to a hexagonal system, being consistent with the ^{19}F NMR and IR data supporting chair type structure [9,10]. Following the Fujii's model, Touhara et al. [11] further investigated the structure of $(C_2F)_n$, with the conclusion that the hexagonal crystal lattice provides several possibilities for various stacking sequences. Using theoretical consideration and numerical calculations, the purpose of this paper is mainly to contribute to elucidation of the latter topic, but also to investigate alternative possibilities connected with the structure and properties of poly(dicarbon monofluoride).

2. Computational details

Here have applied the same method as in Ref. [5], namely the semi-empirical method based on a quasi-relativistic INDO Hamiltonian [12] combined with the cyclic cluster approach [13,14] to treat the three-dimensional periodicity which we have implemented [15] and applied recently [5,16–18]. The method has been shortly described in our study of $(CF)_n$, in this journal [5]. Within the cyclic cluster approach one can treat extremely large finite clusters containing tens of thousands of atoms. This leads to inclusion of the long-range interactions, which in general have significant influence on the electron properties of solid-state systems. The applied (modulo) cyclic boundary condition allows transformation to Bloch orbital basis, and formalism equivalent to the crystal orbital method [19,20], with one to one correspondence between the size of the cyclic cluster and the **k**-points of the first Brillouin zone taken into account. From the physical point of view, all the components (equivalent unit cells) of the generated cluster "feel" the surroundings of the reference (central) cell. We have shown that for sufficiently large cyclic clusters (>5 nm), the bulk is reproduced at least for covalently bound systems. Hence, the density matrix can be safely transformed to any **k**-points of the reciprocal space and full band structure can easily be calculated.

As mentioned above, we shall focus to *trans*-cyclohexane chair layers, and their mutual arrangements that are dominant in the maternal graphite, i.e., the AAAA and the ABAB types of sequences. Various investigated stacking sequences contained either six or 12 atoms per elementary unit cell. With six atom unit cells, we used clusters containing $17 \times 17 \times 17$ duplicates of the reference cell along the respective lattice vectors, i.e., 29478 atoms. In the case of twelve atoms per unit cell, we generated clusters consisting from $15 \times 15 \times 13$ unit cells, i.e., of 35,100 atoms. Such big clusters guaranteed that the resulting electron densities were very close to the bulk limit values.

Geometry optimizations were carried out using the same procedure as in Ref. [5]. We have performed calculations for about 100 points around the expected minima, employed the general form of quadratic energy hypersurface, and used nonlinear simulated annealing method [21], followed by the conjugate gradient optimization [22].

3. Results and discussion

Twelve local minima corresponding to stable structural sequences have been found. These structures are described in Table 1 and in Fig. 1. Energies per C_2F unit, given in Table 2, characterize the thermodynamical stabilities of individual stacking sequences. Most stable are the structures denoted as A6, B3, B5 and B6 whose energies per C_2F unit are fairly close and fall within about 0.6 eV range. Taking into account this fact, statistical distribution of such structures is likely. In such arrangements the maximal entropy contribution leads to the minimum Gibbs energy of the system. This behavior is similar to that in graphite monofluoride, where the real structure seems to be composed from five various stacking sequences [5]. Other investigated sequences of $(C_2F)_n$ are significantly less stabilized, so that their formation during the intercalation of graphite is highly unlikely.

In Table 2 we also display the optimized C–C and C–F bond lengths together with Wiberg indices. In Table 3 other characteristics, such as Mulliken charges, covalency and valency [23] are given. Ranges of the bond lengths between the neighboring carbon atoms ($1.47 \rightarrow 1.55 \times 10^{-10}$ m) and the C–F bonds ($1.41 \rightarrow 1.61 \times 10^{-10}$ m) correspond to covalent bonds

Table 1
Optimized lattice parameters for various stacking sequences of poly(dicarbon monofluoride) (see Fig. 1, all values are in 10^{-10} m)

Config.	Sequence	Mirror symmetry plane	Lattice parameters					
			a	c	z	u	w	v
A1	AAAA	No	2.5832	6.5172	0.002415	0.2499	—	—
A2	AA_xAA_x	No	2.5527	6.8441	0.02386	0.2499	—	—
A3	AA_yAA_y	No	2.5581	6.3405	0.03591	0.2660	0.7143	—
A4	AA′/A′A	Yes	2.5071	6.4545	0.03745	0.2544	0.6816	—
A5	$AA_x/A_x'A'$	Yes	2.5598	13.61923	0.01276	0.1263	0.2555	0.1425
A6	$AA_y/A_y'A'$	Yes	2.5497	13.0382	0.01824	0.1285	0.3452	0.1563
B1	ABAB	No	2.5526	6.6865	0.02332	0.2505	—	—
B2	AB_xAB_x	No	2.5379	6.3020	0.03996	0.2696	0.7155	—
B3	AB_yAB_y	No	2.5490	6.5185	0.03652	0.2573	0.3118	—
B4	AB/B′A′	Yes	2.5550	13.2078	0.01269	0.1275	0.2516	0.3508
B5	$AB_x/B_x'A'$	Yes	2.5477	13.4045	0.01796	0.1255	0.3475	0.1525
B6	$AB_y/B_y'A'$	Yes	2.5471	13.7377	0.0172	0.1241	0.1484	—

in saturated fluorinated hydrocarbons. The charges on fluorine bonding carbon atoms are, as expected, little positive and vary from +0.17e to +0.35e, while being compensated by small negative charges on fluorine atoms that range from –0.15e to −0.23e together with tiny negative charges on the neighboring carbon atoms that do not bond F. These results indicate partial ionic character of the C–F bonds. Weakening of the C–F bonds with respect to C–C is seen as well from the Wiberg indices given in Table 2. Tiny differences between the covalencies, reflecting the covalent character of individual bonds, and the valencies that characterize both covalent and ionic components of all chemical bonds of given atoms [23], clearly confirm the prevailing covalent character even for the C–F bonds.

Band structure calculations have been carried out for all the structures of $(C_2F)_n$ given in Table 1. Results showed that the four most stable structures (A6, B3, B5, B6) are insulators, but some of the optimized structures have conducting properties (A2, A3, A5, B1). If, however, only isolated layers were calculated, the conductivity disappeared, so that it resulted from interlayer interactions. In Figs. 2 and 3 we display the total densities of states (DOS) around the Fermi levels in order to illustrate these facts for the **A** and **B** series of our model structures, respectively. For clarity, we have skipped the identification of DOSs for the improbable (less stable) sequences, which is not important in this context. Additional information about the band gaps is given in Table 4. Hence, according to our study the $(C_2F)_n$ is an insulator, in agreement with experimental observation [1]. Though, some structural sequences could be conducting as a consequence of special interlayer interactions. Such sequences are, however, thermodynamically not favored. Recent band structure calculations on three different models showed conducting behavior [26], too. However, this, more extensive study, shows that the band gaps reflecting the electrical conducting properties strongly depend from the model, but also from the position on the potential energy hypersurface.

Recently, accurate $K\alpha$ X-ray emission spectra ($2p \rightarrow 1s$ transition) both for carbon and fluorine atoms in $(C_2F)_n$ have been measured [27]. These can be—at least qualitatively—compared to the partial densities of the valence $2p$ states from our calculations owing to the final state rule [28]. At the same time the XES spectra are converted to the binding energy scale. As the core $1s$ orbitals in $(C_2F)_n$ are similar to those in $(CF)_n$, we have used the energy shifts due to the binding energies of C $1s$ and F $1s$ from Ref. [27], i.e., 290 eV for C, and 690 eV for F. In Figs. 4 and 5 we compare partial densities of $2p$ states of carbon and fluorine for our most stable configurations A6, B3, B5, and B6, respectively, with the experimental data taken from Ref. [27] in the binding energy scale. For carbon (Fig. 4), one can see that, though the agreement is not perfect, the configurations A6, B3, and B5 exhibit a plateau similar to the experimental finding. B6, however, exhibits a peak at about –6 eV that can hardly be identified on the experimental curve. This might lead to a conclusion that B6 configuration (though most stable in our calculations) is not be preferred in real $(C_2F)_n$. However, if we have simply averaged the values from all these configurations (curve **1**), we obtained reasonable agreement with the experimental curve. With an exclusion of B6, not very much was changed. Also from Fig. 5 one sees that the averaged values from all the structures give rise to relatively nice agreement with the experimental finding. For individual structures this was not true.

4. Conclusions

Results of the calculation of the structural and electronic properties of the poly(dicarbon monofluoride) performed in this work can be summarized as follows:

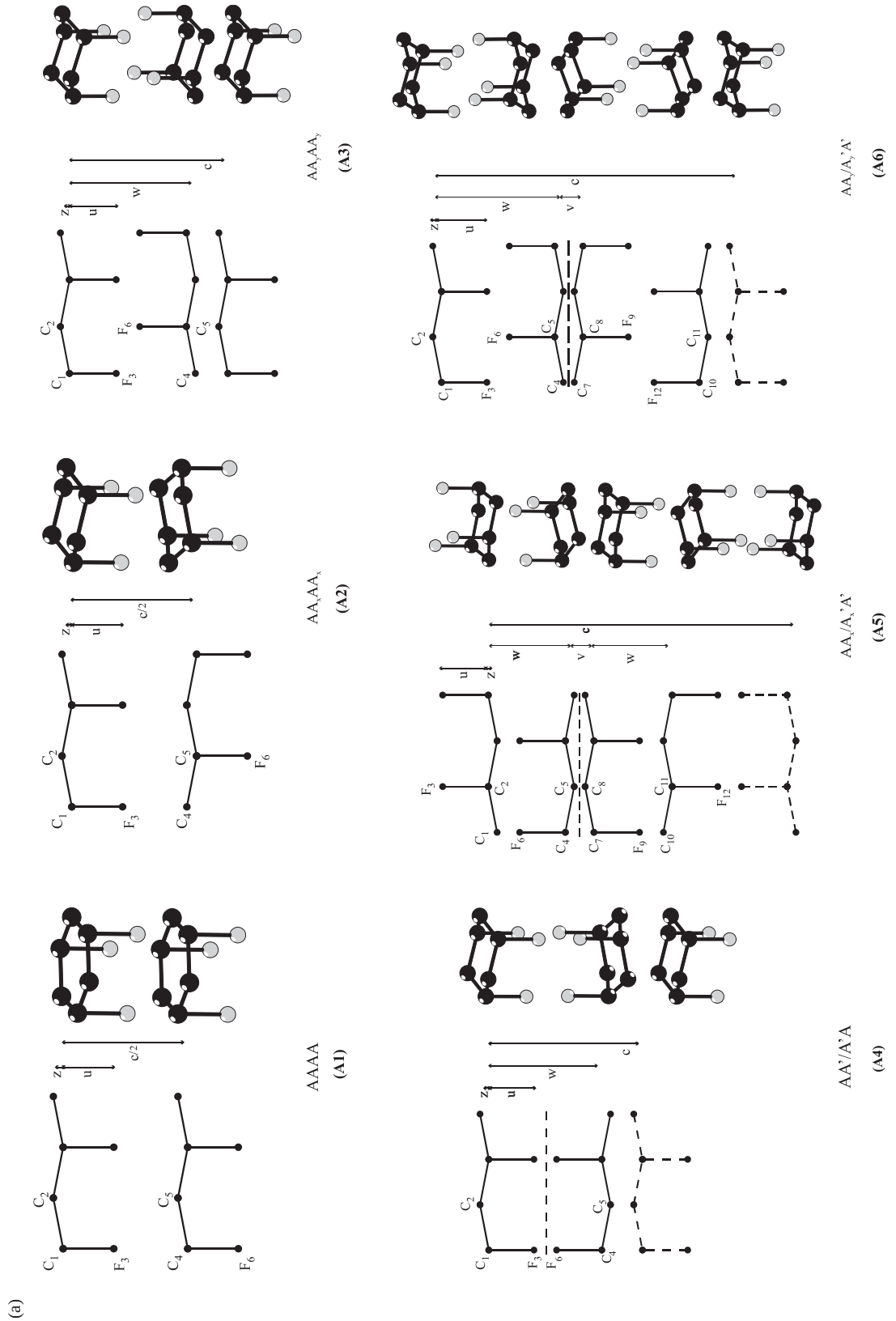
(a)
AAAA
(A1)
AA$_x$AA$_x$
(A2)
AA$_y$AA$_y$
(A3)
AA'/A'A
(A4)
AA$_x$/A$_x$'A'
(A5)
AA$_y$/A$_y$'A'
(A6)
C1
C2
C4
C5
C7
C8
C10
C11
F3
F6
F9
F12
u
w
v
c
c/2
z

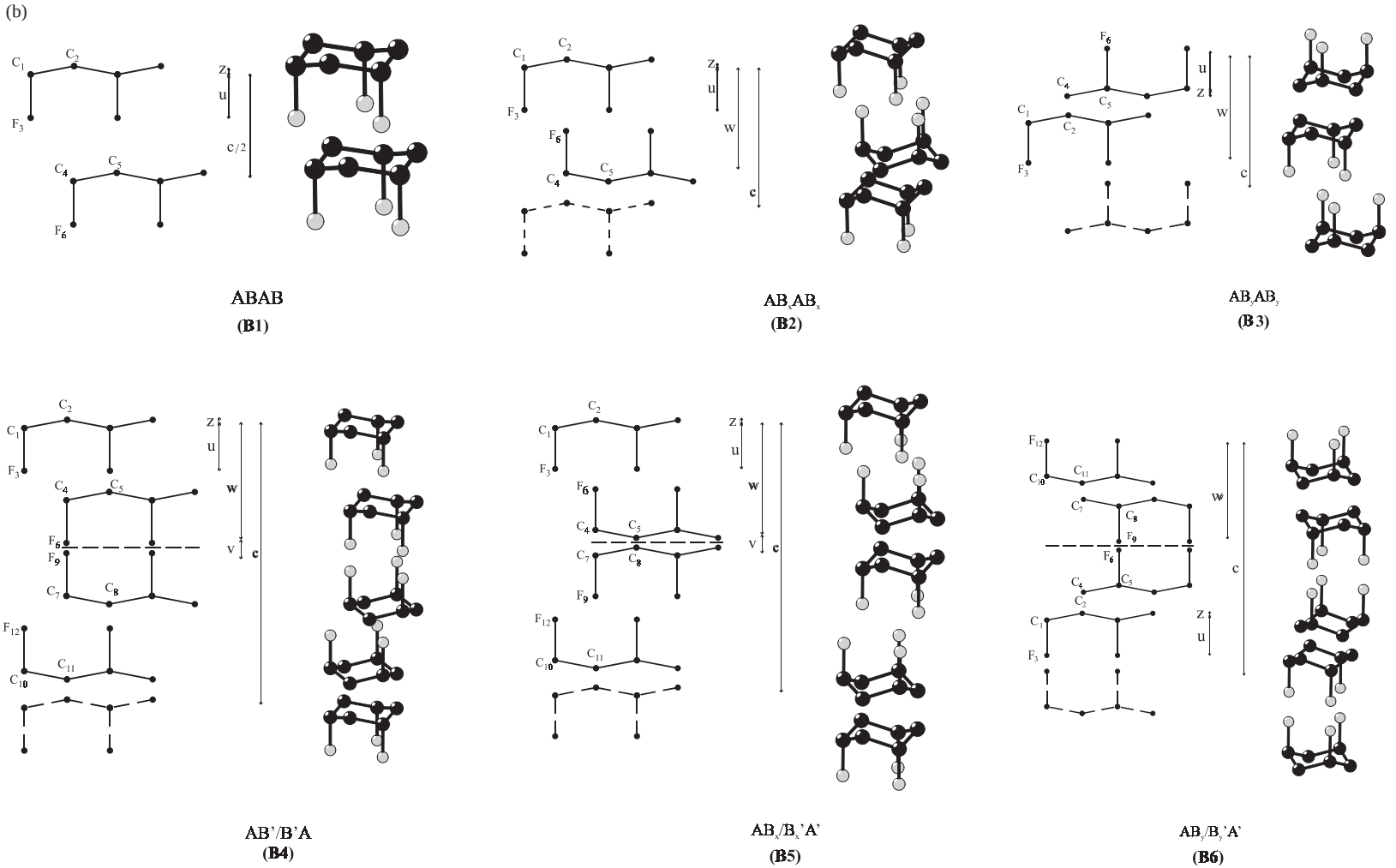

Fig. 1. Schematic pictures of the basic motifs for the apparently stable (local minima) stacking sequences of the poly(dicarbon monofluoride) in the hexagonal lattice. Lattice parameters are given in Table 1, *a* corresponds to the closest distance between the two neighboring fluorine atoms in a layer, the meaning of other parameters (in *c* direction) is shown on the projections of the nearest atoms to the *a*–*c* planes, as given on the left side for each structure.

Table 2
Energies per C_2F unit relative to the most stable structure B6 (ΔE), bond distances (in 10^{-10} m) and Wiberg indices of individual bonds for stacking sequences defined in Table 1

Sequence	Config.	ΔE (eV)	d_{C1-C2}	d_{C2-C3}	d_{C1-F}	W_{C1-C2}	W_{C1-F}
AAAA	A1	7.58	1.49	1.49	1.61	1.07	0.38
AA_xAA_x	A2	3.79	1.51	1.47	1.55	1.05	0.43
AA_yAA_y	A3	4.11	1.55	1.48	1.46	0.93	0.76
AA′/A′A	A4	5.38	1.53	1.54	1.40	0.95	0.88
$AA_x/A_x'A'$	A5	2.23	1.52	1.54	1.59	1.08	0.48
$AA_y/A_y'A'$	A6	0.57	1.55	1.47	1.44	0.95	0.88
ABAB	B1	5.00	1.51	1.47	1.52	1.00	0.76
AB_xAB_x	B2	4.19	1.55	1.47	1.45	0.92	0.87
AB_yAB_y	B3	0.53	1.55	1.47	1.44	0.95	0.88
AB/B′A′	B4	3.39	1.51	1.48	1.52	0.97	0.81
$AB_x/B_x'A'$	B5	0.62	1.55	1.47	1.44	0.95	0.88
$AB_y/B_y'A'$	B6	0.00	1.55	1.47	1.47	0.96	0.80

Table 3
Charges and bond characteristics of individual atoms in optimal geometries

Sequence	Conf.	q_{C1}	q_{C-0}	q_F	Covalency			Valency		
					C_1	C_2	F	C_1	C_2	F
AAAA	A1	0.31	−0.08	−0.24	3.95	3.95	1.04	3.97	3.97	1.11
AA_xAA_x	A2	0.19	−0.05	−0.14	3.98	3.99	1.20	3.98	3.99	1.22
AA_yAA_y	A3	0.35	−0.08	−0.26	3.94	3.97	1.04	3.97	3.97	1.11
AA′/A′A	A4	0.21	−0.06	−0.15	3.95	3.98	1.15	3.97	3.98	1.20
$AA_x/A_x'A'$	A5	0.12	−0.02	−0.09	3.99	3.99	1.20	3.99	3.99	1.20
$AA_y/A_y'A'$	A6	0.31	−0.11	−0.20	3.95	3.98	1.06	3.98	3.98	1.09
ABAB	B1	0.23	−0.05	−0.19	3.97	3.99	1.12	3.98	3.99	1.17
AB_xAB_x	B2	0.27	−0.10	−0.17	3.97	3.96	1.07	4.00	3.96	1.12
AB_yAB_y	B3	0.27	−0.07	−0.20	3.96	3.98	1.06	3.96	4.00	1.10
AB/B′A′	B4	0.26	−0.09	−0.18	3.96	3.98	1.08	3.98	3.98	1.11
$AB_x/B_x'A'$	B5	0.29	−0.09	−0.20	3.95	3.98	1.05	3.98	3.98	1.09
$AB_y/B_y'A'$	B6	0.17	−0.05	-0.12	3.98	3.98	1.13	3.99	3.98	1.15

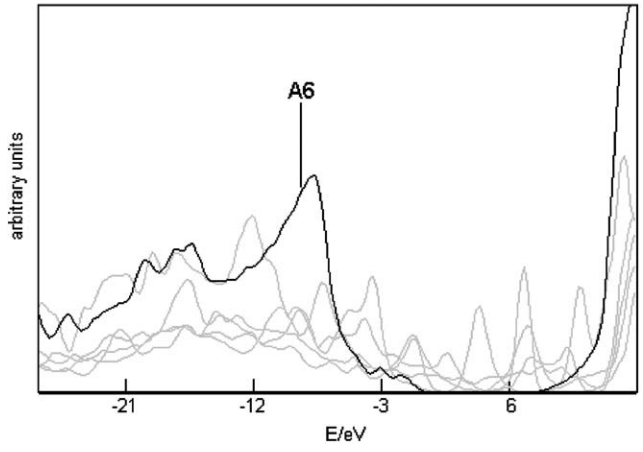

Fig. 2. DOS in the vicinity of Fermi level (varies around 0) for different structures of the AAAA sequences of the poly(dicarbon monofluoride)—series **A** defined in Table 1 and Fig. 1. Grey lines correspond to structures A1–A5 that are unlikely, therefore those are only given for comparison with much more stable structure A6 (black).

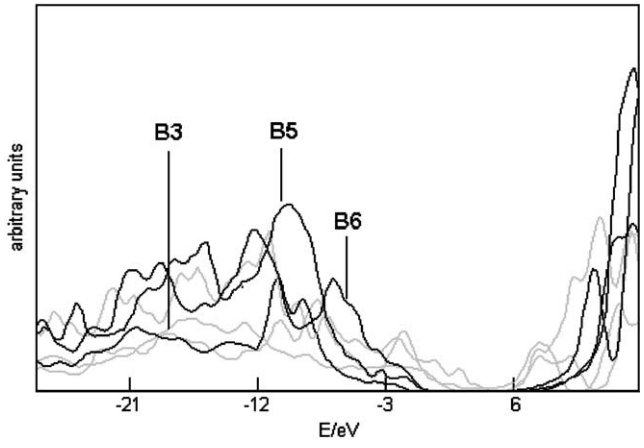

Fig. 3. Calculated total DOS in the vicinity of Fermi level (varies around 0) for different structures of the ABAB sequences of the poly(dicarbon monofluoride)—series **B** defined in Table 1 and Fig. 1. Grey lines correspond to structures B1, B2, and B4 that are unlikely, therefore those are only given for comparison with much more stable structures B3, B5 and B6 (black).

Table 4
Differences between the energies of the valence and conductive bands for the stacking sequences defined in Table 1 (energies are in eV)

Sequence	Configuration	Band gap	Band gap corrected[a]	k-Point[b]
AAAA	A1	2.28	1.57	K
AA_xA_x	A2	—	metal	Γ[c]
AA_yAA_y	A3	—	metal	Γ[c]
AA/A′A	A4	4.28	3.88	A
$AA_x/A_x'A'$	A5	—	metal	Γ[c]
$AA_y/A_y'A'$	A6	9.04	8.52	Γ
ABAB	B1	—	metal	A[c]
AB_xAB_x	B2	4.57	3.94	H
AB_yAB_y	B3	8.27	8.90	A
AB′/B′A	B4	2.45	1.76	K, H
$AB_x/B_x'A'$	B5	9.03	8.52	Γ
$AB_y/B_y'A'$	B6	6.82	6.31	Γ

[a] Corrected band gaps using improved virtual space [24].
[b] The notation for the symmetry points of the first Brillouin zone is taken from Ref. [25].
[c] The point with maximal overlap between the valence and conductive band.

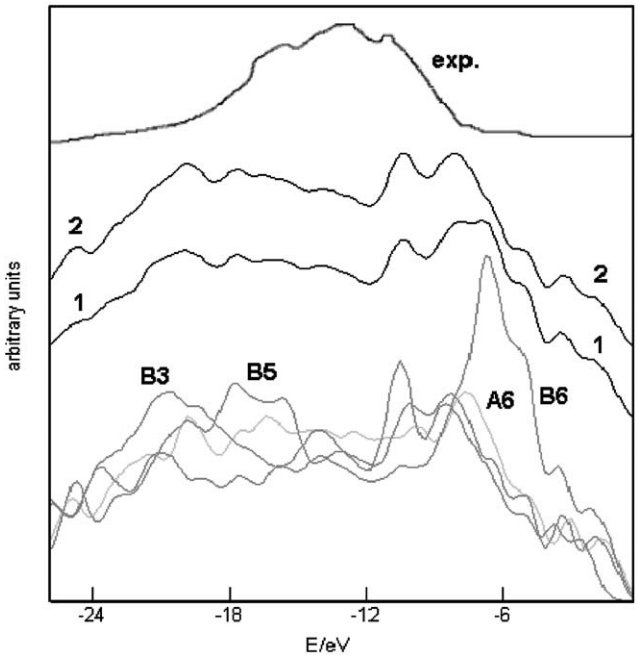

Fig. 4. Calculated partial densities of 2*p* valence states of the carbon atoms for selected (most stable) structures of poly(dicarbon monofluoride) compared with the experimental C *Kα* XES spectrum in the binding energy scale [27]. **1**—the average of A6, B3, B5 and B6; **2**—the average of A6, B3, and B5.

- The poly(carbon monofluoride) creates a layered structure with puckered individual layers built of *trans*-cyclohexane chairs. Resulting structure forms a hexagonal crystal lattice.
- We have found 12 stacking sequences of AAAA and ABAB types that can be considered as stable. Four of those are thermodynamically much more favored, namely configurations A6, B3, B5, and B6 from Table 1. Their energies per C_2F unit differ within 0.6 eV only. Consequently, in the real poly(dicarbon monofluoride), the statistical distribution of these four structures can be expected. As well, simple averaging of the partial densities of 2*p* states agrees with the experimental XES data much better than separately for each configuration. In such arrangements the maximum entropy contribution leads to the minimum Gibbs energy of the system.
- Intercalated fluorine atoms form strong covalent, weakly polarized, bonds with carbon atoms of the maternal layer, as expected.
- The band structure calculations showed that the most stable sequences (which form real poly(carbon monofluoride)) have insulating properties, and so, in accordance with the experimental measurements, the real $(C_2F)_n$ is an insulator.
- Nevertheless, some of the less stable structural sequences show conducting properties, which disappeared when a mere single layer was considered. This, undoubtedly, confirms that the conductivity is caused by interlayer interactions.

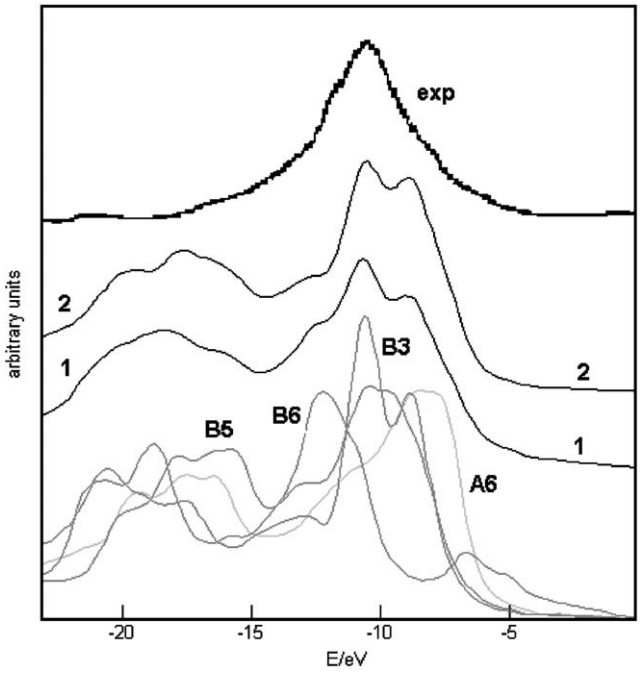

Fig. 5. Calculated partial densities of 2*p* valence states of the fluorine atoms for selected (most stable) structures of poly(dicarbon monofluoride) compared with the experimental F *Kα* XES spectrum in the binding energy scale [27]. **1**—the average of A6, B3, B5 and B6; **2**—the average of A6, B3, and B5.

Acknowledgments

The authors express cordial thanks to Dr. E. Hubinak from SFC, Inc., and Slovak Grant Agency VEGA

(Contracts No. 1/9255/02, and 2/7203/20) for supporting this project.

References

[1] V.T. Nakajima, N. Watanabe, Graphite Fluorides and Carbon–Fluorine Compounds, CRC Press, Boca Raton, FL, 1991.
[2] A. Hamwi, M. Daoud, J.C. Cousseins, Synth. Metals 30 (1989) 23.
[3] N. Watanabe, Solid State Ionics 1 (1980) 87.
[4] M. Fukuda, T. Iijima, in: J.P. Gabano (Ed.), Lithium Batteries, Academic Press, London, 1983.
[5] A. Zajac, P. Pelikán, J. Minár, J. Noga, M. Straka, P. Baňacký, S. Biskupič, J. Solid State Chem. 150 (2000) 286.
[6] R.L. Fusaro, H.E. Sliney, A. S. L. E. Trans. 13 (1970) 56.
[7] Y. Kita, N. Watanabe, Y. Fujii, J. Am. Chem. Soc. 101 (1979) 3822.
[8] Y. Fujii, Structure of $(C_2F)_n$, Master's Thesis, Kyoto University, Kyoto, 1979.
[9] L.B. Ebert, J.I. Brauman, R.A. Huggins, J. Am. Chem. Soc. 96 (1974) 7841.
[10] T. Nakajima, M. Kawaguchi, N. Watanabe, Carbon 20 (1982) 287.
[11] H. Touhara, K. Kadono, Y. Fujii, N. Watanabe, Z. Anorg. Allg. Chem. 544 (1987) 7.
[12] R. Boča, Int. J. Quantum Chem. 31 (1987) 941;
R. Boča, Int. J. Quantum Chem. 34 (1988) 385.
[13] Deák, Acta Phys. Acad. Sci. Hung. 50 (1981) 247;
Deák, Acta Phys. Status Solidi 217 (2000) 9.
[14] R.A. Evarestov, Th. Bredow, K. Jug, Phys. Solid State 43 (2001) 1774.
[15] P. Baňacký, S. Biskupič, J. Noga, P. Noga, P. Pelikán, A. Zajac, SOLID2000—A Program System Designed for Calculation of the Electronic Structure of Solid State Systems, S-tech Inc., Bratislava, 2000; www.stech.sk
[16] J. Noga, P. Baňacký, S. Biskupič, R. Boča, P. Pelikán, M. Svrček, A. Zajac, J. Comput. Chem. 20 (1999) 253.
[17] A. Zajac, P. Pelikán, J. Noga, P. Baňacký, S. Biskupič, M. Svrček, J. Phys. Chem. 104 (2000) 1708.
[18] P. Pelikán, M. Košuth, S. Biskupič, J. Noga, M. Straka, A. Zajac, P. Baòacký, Int. J. Quantum Chem. 157 (2001) 168.
[19] J.M. André, L. Gouverneur, G. Leroy, Int. J. Quantum Chem. 1 (1967) 427;
J.M. André, L. Gouverneur, G. Leroy, Int. J. Quantum Chem. 1 (1967) 451.
[20] G. Del Re, J. Ladik, G. Biczó, Phys. Rev. 155 (1967) 997.
[21] V. Kvasnička, J. Pospíchal, Intell. Lab. Syst. 39 (1997) 161.
[22] W.H. Press, S.A. Teukolsky, W.T. Vetterling, B.B. Flammery, Numerical Recipes in FORTRAN, Cambridge University Press, Cambridge UK, 1992.
[23] A. Veryazov, A.V. Leko, R.A. Evarestov, Phys. Solid State 41 (1999) 1286.
[24] S. Huzinaga, C. Arnau, Phys. Rev. 54 (1971) 1948.
[25] C.J. Bradley, A.P. Cracknell, The Mathematical Theory of Symmetry in Solids, Claredon Press, Oxford, 1972.
[26] L.G. Bulusheva, S.L. Kasyanov, A.V. Okotrub, Phys. Low-Dimens. Struct. 12 (1998) 189.
[27] E.Z. Kurmaev, A. Moewes, D.L. Ederer, H.L. Ishii, K. Seki, M. Yanagihara, F. Okino, H. Touhara, Phys. Lett. A 288 (2001) 340.
[28] U. von Barth, G. Grossmann, Phys. Rev. B 25 (1982) 5150.